World Academy of Science, Engineering and Technology
International Journal of Computer and Information Engineering
Vol:11, No:7, 2017

Sparse Unmixing of Hyperspectral Data by Exploiting Joint-Sparsity and Rank-Deficiency

Fanqiang Kong, Chending Bian

***Abstract*—**In this work, we exploit two assumed properties of the abundances of the observed signatures (endmembers) in order to reconstruct the abundances from hyperspectral data. Joint-sparsity is the first property of the abundances, which assumes the adjacent pixels can be expressed as different linear combinations of same materials. The second property is rank-deficiency where the number of endmembers participating in hyperspectral data is very small compared with the dimensionality of spectral library, which means that the abundances matrix of the endmembers is a low-rank matrix. These assumptions lead to an optimization problem for the sparse unmixing model that requires minimizing a combined $l_{2,p}$-norm and nuclear norm. We propose a variable splitting and augmented Lagrangian algorithm to solve the optimization problem. Experimental evaluation carried out on synthetic and real hyperspectral data shows that the proposed method outperforms the state-of-the-art algorithms with a better spectral unmixing accuracy.

***Keywords*—**Hyperspectral unmixing, joint-sparse, low-rank representation, abundance estimation.

I. Introduction

WITH the rapid development of space technology, hyperspectral imaging (HSI) has been widely applied to various fields such as environmental monitoring, resource survey, and target detection [1]. Due to the insufficient spatial resolution of the hyperspectral remote sensors, some pixels of the hyperspectral image often contain a mixture of distinct materials. In order to deal with the great challenging task, the hyperspectral unmixing technique was proposed to decompose each pixel's spectrum to identify the pure constituent spectra (endmembers) and estimate the abundances of the endmembers in the mixed pixel. The nonlinear mixture model (NLMM) and the linear mixture model (LMM) are two basic hyperspectral unmixing models, which we use to analyze the mixed pixel problem [12]. Under the LMM, several hyperspectral unmixing approaches based on statistics [2], [3], geometry [2], [4], and nonnegative matrix factorization [5] have been proposed. However, some of these methods [2]-[4] assume that the hyperspectral data contain at least one pure pixel per endmember. If the pure pixel assumption is not fulfilled, these methods are very likely to fail.

Sparse unmixing, as a semi-supervised linear spectral unmixing approach, has been proposed to overcome this difficulty. It assumes that the measured pixels can be expressed as a linear combination of a few spectral endmembers from the spectral library that is known a priori [6], [12]. Several sparse regression techniques, such as greedy algorithms (GAs) [7] and convex relaxation methods [8]-[10], are usually adopted to solve the sparse unmixing problem. Convex relaxation methods, such as SUnSAL [8], SUnSAL-TV [9], and CLSUnSAL [10], use the alternating direction method of multiples (ADMM) to solve the constrained l_1 norm regression problem efficiently. The GAs, such as OMP [6] and SP, can get an approximate solution for the l_0 norm problem without smoothing the penalty function and have low computational complexity.

In this paper, we consider incorporating joint-sparse and low-rank representation into the sparse unmixing model, thus exploiting joint-sparsity and rank-deficiency information in hyperspectral images. Then, a novel cost function is proposed comprising a least-squares optimization problem which is regularized by the non-convex $l_{2,p}$ -norm as the sparsity penalty and the nuclear norm as the low-rank penalty. We introduce a new sparse unmixing algorithm, which is termed sparse unmixing via joint-sparse and low-rank representation (SUnJSLRR), to solve this optimization problem. The experiments were carried out on three simulated hyperspectral datasets and one real hyperspectral dataset. It was found that the proposed method yields the best spectral unmixing accuracy in terms of quantitative evaluation.

II. Simultaneous Sparse Unmixing Model

The LMM assumes that the measured spectrum vector of a mixed pixel can be expressed as a linear combination of only a few spectral signatures present in a known spectral library. Let $y \in R^L$ be the measured vector of the mixed pixel with L bands, $A \in R^{L \times m}$ is a $L \times m$ spectral library, and m is the number of endmembers in the spectral library A, then the linear sparse unmixing model can be expressed as:

$$y = Ax + n \tag{1}$$

The simultaneous sparse unmixing model expresses that several mixed pixels can be expressed as different linear combinations of the same spectral signatures in the spectral library. A similar sparsity pattern acts as a priori information, which improves the conditioning of the sparse regression problem. Then, the linear sparse unmixing model can be represented as a multiple measurement vectors (MMV) model:

$$Y = AX + N \tag{2}$$

where $Y \in R^{L \times K}$ denotes the hyperspectral data matrix with L

F. Kong and C. Bian are with College of Astronautics, Nanjing University of Aeronautics and Astronautics, Nanjing, 210016, China (e-mail: kongfq@nuaa.edu.cn, 1065286194@qq.com).

bands and K mixed pixels, $A \in R^{L\times m}$ is the spectral library, $X \in R^{m\times K}$ is the fractional abundance matrix, where each column represents the abundance fractions of a mixed pixel. Under the simultaneous sparse unmixing model, the simultaneous sparse unmixing problem becomes as:

$$\min_X \|X\|_{2,1} \quad s.t. \|Y - AX\|_F \le \delta, X \ge 0 \tag{3}$$

where $\|X\|_{2,1} = \sum_{i=1}^{m} \|X_i\|_2$ denotes the $l_{2,1}$ norm of X, X_i denotes the ith row of X. In [10], collaborative SUnSAL (CLSUnSAL), which is also based on the ADMM, has been proposed to solve it.

III. Proposed Hyperspectral Unmixing Methodology

In this work, we exploit two assumed properties of the abundances of the observed endmembers for the sparse umixing model. Joint-sparsity is the first property of the abundances, which assumes a few adjacent pixels can be expressed as different linear combinations of some same signatures in the spectral library. So, we employ the joint-sparsity regularizer to enforce structured sparsity on the abundance coefficients. To exploit the abundance structure of the endmembers, we also employ the low-rank representation model to enforce rank-deficiency on the abundance coefficients. Reformulating the constrained optimization problem (3) with the joint-sparsity and the low-rank regularizer, we get

$$\min_X \lambda_S \|X\|_{2,p} + \lambda_L \|X\|_* \quad s.t. \|Y - AX\|_F \le \delta, X \ge 0 \tag{4}$$

where $\|X\|_* = tr(\sqrt{X^T X}) = \sum_{k=1}^{rank(X)} \sigma_i(X)$, denotes the nuclear norm of X, $\sigma_i(X)$ is the ith largest singular value of X, $rank(X)$ is the rank of X, the parameter λ_S and λ_L are the regularization parameters controlling the weight of joint-sparsity and low-rank terms.

The optimization problem in (8) can be rewritten in the following equivalent form by minimizing the respective Lagrange function:

$$\min_X \frac{1}{2}\|Y - AX\|_F^2 + \lambda_S \|X\|_{2,p} + \lambda_L \|X\|_* + \iota_{R+}(X) \tag{5}$$

where the term $l_{\{R+\}}(\boldsymbol{X})$ denotes the ANC function: $l_{\{R+\}}(\boldsymbol{X})$ is zero if $\boldsymbol{X} \ge \boldsymbol{0}$ is satisfied and $+\infty$ otherwise.

The optimization problem in (5) can be written in a compact form as:

$$\min_X \frac{1}{2}\|Y - AX\|_F^2 + \lambda_S \|X\|_{2,p} + \lambda_L \|V\|_* + \iota_{R+}(V) \quad s.t. V = X \tag{6}$$

The augmented Lagrangian of problem (6) is

$$L(X,V,D) = \frac{1}{2}\|Y - AX\|_F^2 + \lambda_S \|X\|_{2,p} + \lambda_L \|V\|_* + \iota_{R+}(V) + \frac{\mu}{2}\|X - V - D\|_F^2 \tag{7}$$

where $\mu > 0$ is a positive constant representing the Lagrange multiplier, V and D are the intermediate variables. To solve (7), the optimal problem of (7) is decomposed into a sequence of simpler ones via the alternating direction method of multipliers (ADMM), which are defined as:

$$(X^{(k+1)}, V^{(k+1)}) = \arg\min_{X,V} L(X,V) \tag{8}$$

$$D^{(k+1)} = D^{(k)} - (X^{(k+1)} - V^{(k+1)}) \tag{9}$$

Firstly, we need to achieve the solution X of the augmented Lagrange problem. The terms of the objective function (7) which do not contain the variable X are not considered, so the reduced optimization problem of the variable X can be written as:

$$X^{(k+1)} = \arg\min_X \frac{1}{2}\|Y - AX\|_F^2 + \lambda_S \|X\|_{2,p} + \frac{\mu}{2}\|X - V - D\|_F^2 \tag{10}$$

It is evident that the minimization problem (10) is still hard to solve efficiently in a direct way, since it involves a $l_{2,p}$ -norm terms. To solve this problem, we follow the M-FOCUSS algorithm [11] to derive the solution with good theoretical guarantee of correctness.

Since the partial derivative of $\|X\|_{2,p}$ with respects to an entry $x_{m,n}$ is:

$$\frac{\partial \|X\|_{2,p}}{\partial x_{m,n}} = \frac{\partial}{\partial x_{m,n}} \sum_i (\sum_j x_{i,j}^2)^{p/2} = p \|x_{m,\cdot}\|_2^{p-2} x_{m,n} \tag{11}$$

Then, the gradient of $\|X\|_{2,p}$ writes:

$$\frac{\partial \|X\|_{2,p}}{\partial X} = diag(p \|x_{m,\cdot}\|_2^{p-2}) X \tag{12}$$

Using (12), the gradient of the objective function (10) writes:

$$-A^T(Y - AX) + \lambda_S PX + \mu(X - V - D) = 0 \tag{13}$$

where $P = diag(p \|x_{m,\cdot}\|_2^{p-2})$, and the weighting matrix W is defined as $W = diag(p^{-1/2} \|x_{m,\cdot}\|_2^{1-p/2})$, $W^{-2} = P$.

After simple algebras, the solution of (10) is

$$X^{(k+1)} = W((AW)^T(AW) + (\lambda_S + \mu W^T)I)^{-1}((AW)^T Y + \mu W^T(V + D)) \quad (14)$$

To compute $V^{(k+1)}$, the optimization problem can be solved as:

$$V^{(k+1)} = \min_V \lambda_L \|V\|_* + \iota_{R+}(V) + \frac{\mu}{2}\left\|X^{(k+1)} - V - D^{(k)}\right\|_F^2 \quad (15)$$

Considering the nonnegative constraint function $\iota_{R+}(\cdot)$, we can firstly solve the following optimization problem for the variable Z. Then, the variable Z is projected onto the non-negative orthant, thus $V^{(k+1)} \leftarrow \max(Z, 0)$.

$$Z = \min_V \lambda_L \|Z\|_* + \frac{\mu}{2}\left\|X^{(k+1)} - Z - D^{(k)}\right\|_F^2 \quad (16)$$

The solution of (16) can be easily solved by the singular value shrinkage[26]:

$$Z^{(k+1)} = S_{\lambda_L/\mu}(X^{(k+1)} - D^{(k)}) \quad (17)$$

where the singular value shrinkage is defined by

$$S_\tau(Q) = U(\sum - diag(\tau))_+ V^T \quad (18)$$

where U, V, and $\sum$ are the singular vectors and values of Q, and $(x)_+ = \max\{x, 0\}$.

IV. Experimental Results

In this section, we conduct both simulated hyperspectral data and real hyperspectral data to evaluate the effectiveness of the proposed algorithm. The proposed algorithm is compared with SUnSAL and CLSUnSAL. All the considered algorithms have taken into account the abundance nonnegativity constraint. The signal-to-reconstruction error (SRE) is used to assess the quality of the reconstruction of spectral mixtures.

A. Evaluation with Simulated Data

In the simulated experiments, the spectral library A was generated by using the United States Geological Survey (USGS) digital spectral library (splib06a), which contains 498 spectral signatures with reflectance values given in 224 spectral bands between the interval of 0.4 μm and 2.5 μm. Using the spectral library A, we generated three datacubes of 50×50 pixels and 224 bands per pixel, each containing a different number of endmembers: $k_1 = 4$ (denoted by DC1), $k_2 = 6$ (DC2), $k_3 = 8$ (DC3). The endmembers were randomly selected from the spectral library A. The fractional abundances of the endmembers selected from the spectral library were generated randomly, using a Dirichlet distribution. After the simulated datacubes were generated, Gaussian white noise was added to the simulated datacubes, having three levels of the signal-to-noise ratio (SNR), i.e. 20, 30, and 40 dB.

Table I shows the SRE (dB) obtained by the different tested methods with the three considered datacubes, using three SNR levels. The SREs of all the algorithms increase as the SNR increases. From Table I, we can find that the proposed method and CLSUnSAL perform better than SUnSAL in all the cases. This result indicates that the proposed method and CLSUnSAL, imposing joint-sparsity on the abundance coefficients of the endmembers for all pixels, can obtain a higher accuracy than SUnSAL. In all the cases, the proposed method behaves better than CLSUnSAL. This observation indicates that the non-convex $l_{2,p}$ -norm and nuclear norm can get better recovery results than the convex $l_{2,1}$ -norm. For high SNR values, the improvements of SREs obtained by the proposed method are significant, with regard to CLSUnSAL and SUnSAL. This is due to the fact that, the proposed method, using the $l_{2,p}$ -norm and nuclear norm to enforce joint-sparsity and rank-deficiency on the abundance coefficients, is able to recover the fractional abundances with good accuracy.

TABLE I
SRE Values Obtained by Different Unmixing Methods

Data cube	SNR	SRE (dB)		
		SUnSAL	CLSUnSAL	SUnJSLRR
DC1	20dB	2.098	3.105	**9.113**
	30dB	7.1615	10.3514	**22.348**
	40dB	15.0799	20.3994	**36.5292**
DC2	20dB	1.842	3.063	**6.27**
	30dB	6.213	7.736	**18.2016**
	40dB	13.552	19.315	**31.3057**
DC3	20dB	1.281	2.386	**3.7196**
	30dB	4.902	6.739	**14.7291**
	40dB	10.728	17.297	**26.2334**

For visual comparison, Fig. 1 shows the estimated fractional abundances of the considered unmixing methods in DC2 with SNR of 30 dB, along with the ground-truth abundance. In order to better visualization, the same abundances of 100 randomly selected pixels are shown. From Fig. 2, we can find that the estimated abundances by SUnSAL contain more noise points compared with CLSUnSAL and the proposed method. Compared with CLSUnSAL, the proposed method that considers joint-sparsity and low-rank information can achieve a better visual effect and contain fewer noise points.

B. Evaluation with Real Data

We use the AVIRIS Cuprite dataset as the hyperspectral dataset in our real data experiment. The size of the real data cube is a 250×191 pixels subset with 188 spectral bands; water absorption bands and low SNR bands were removed. The spectral library for this dataset is the USGS spectral library (contains 498 pure signatures), in which corresponding bands were removed. For illustrative purposes, Fig. 2 shows a qualitative comparison among the fractional abundance maps of three different materials (alunite, buddingtonite, and chalcedony) estimated by all the algorithms. From Fig. 2, the abundances estimated by SUnJSLRR are comparable or higher

in the regions assigned to the respective minerals in comparison to SUnSAL and CLSUnSAL, with regard to the classification maps produced by the Tricorder3.3 software.

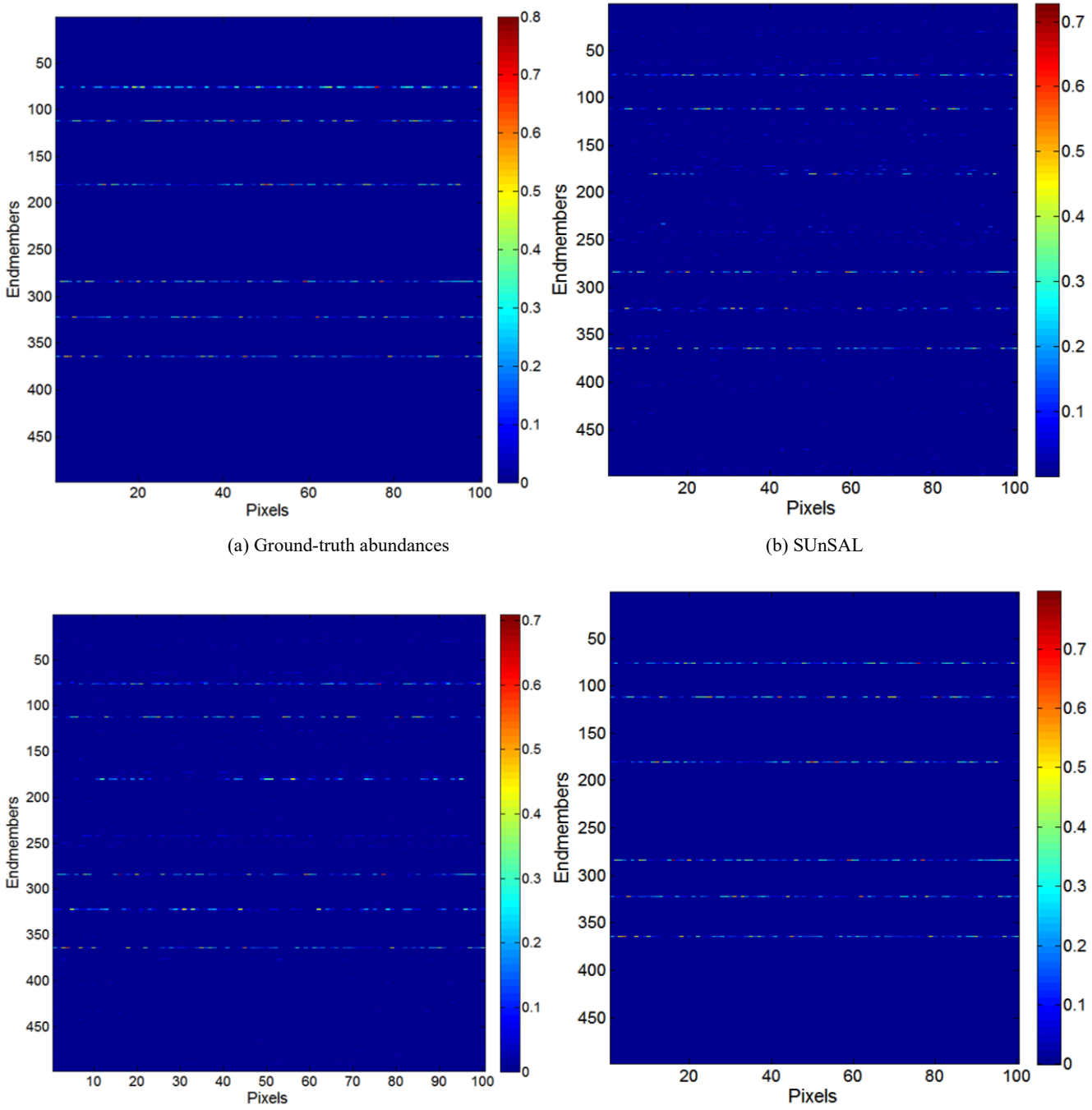

(a) Ground-truth abundances (b) SUnSAL

(c) CLSUnSAL (d) SUnJSLRR

Fig. 1 Ground-truth and estimated abundance in DC2 with 30 dB white noise

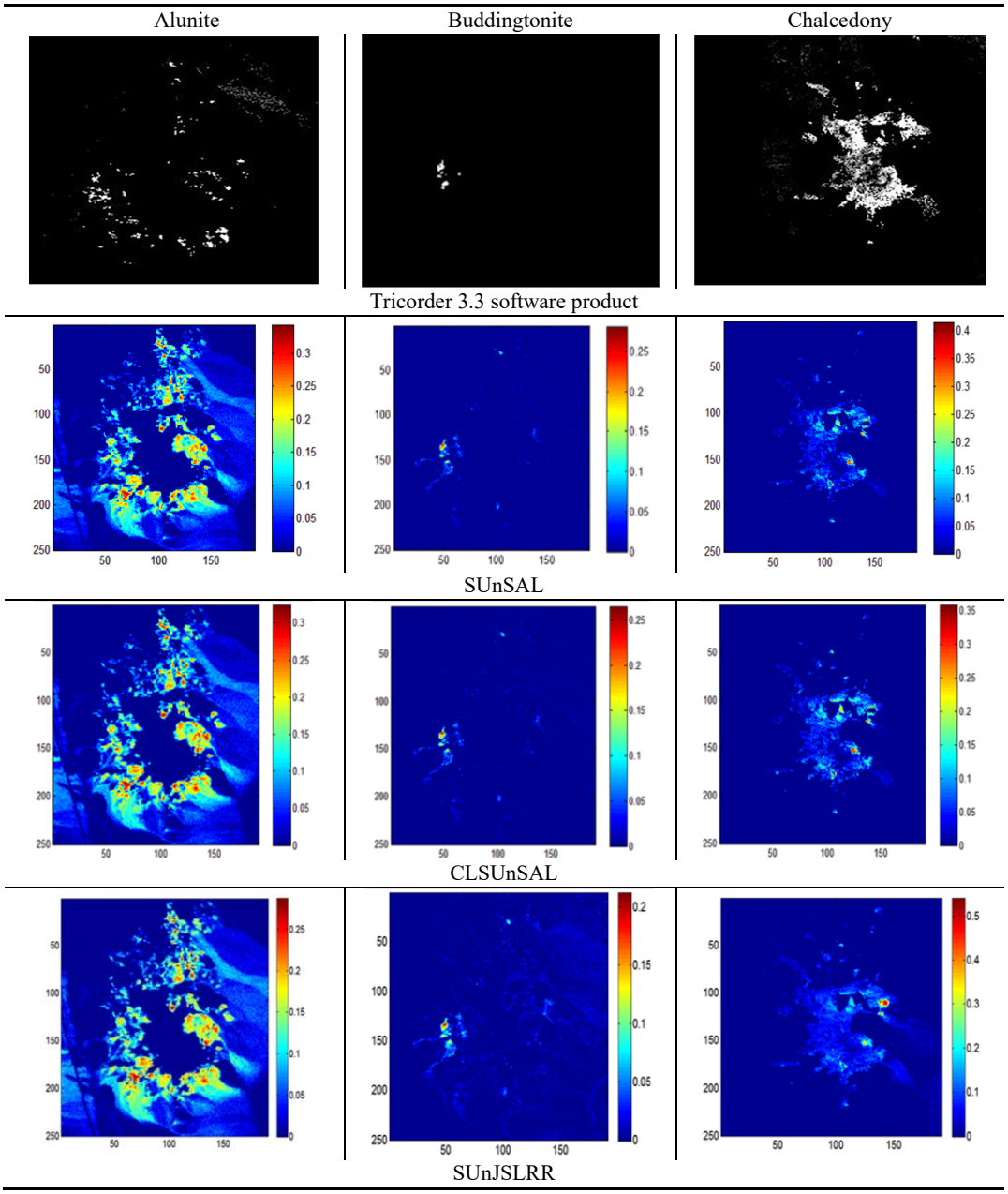

Fig. 2 Abundance maps estimated for the minerals: *alunite*, *buddingtonite*, and *chalcedony* by applying the different algorithms

V. Conclusion

In this paper, we employ joint-sparse and low-rank representation to exploit the spatial structure of the abundance vectors for sparse unmixing. Then, we propose a novel sparse unmixing model to exploit two assumed properties of the abundances vectors. Based on the sparse unmixing model, we formulate an optimization problem that minimizes a combination of the $l_{2,p}$ -norm and the nuclear norm. Then, we present a new algorithm, which is called SUnJSLRR, to solve this optimization problem. Three simulated hyperspectral datasets and one real hyperspectral dataset were used to evaluate the performance of the proposed SUnJSLRR. The experimental results show that the proposed method significantly outperforms SUnSAL and CLSUnSAL.

Acknowledgment

The authors would like to thank M.-D. Iordache, J. Bioucas-Dias, and A. Plaza for sharing their codes for the algorithms of CLSUnSAL and SUnSAL.

This work has been supported by a grant from the National Natural Science Foundation of China (61401200).

References

[1] G. Shaw and D. Manolakis, "Signal processing for hyperspectral image exploitation", IEEE Signal Process. Mag., vol.19, no.1, pp.12–16, 2002.

[2] J. M. Bioucas-Dias, A. Plaza, N. Dobigeon, M. Parente, Q. Du, P. Gader, and J. Chanussot, "Hyperspectral unmixing overview: Geometrical, statistical, and sparse regression-based approaches", IEEE J. Sel.Topics

Appl. Earth Observ. Remote Sens., vol.5, no. 2, pp. 354-379, 2012.
[3] M. Arngren, M. N. Schmidt, and J. Larsen, "Bayesian nonnegative matrix factorization with volume prior for unmixing of hyperspectral images", in Proc. IEEE Int. Workshop MLSP, France: Grenoble, 2009, pp. 1-6.
[4] H. Pu, B. Wang, L. Zhang, "Simplex geometry-based abundance estimation algorithm for hyperspectral unmixing", Scientia Sinica Infor-mationis, vol.42, no.8, pp.1019-1033, 2012.
[5] Y. Qian, S. Jia, J. Zhou, et al. "Hyperspectral unmixing via sparsity-constrained nonnegative matrix factorization". Geoscience and Remote Sensing, IEEE Transactions on, 2011, vol.49, no.11, pp.4282-4297.
[6] M.-D. Iordache, J. Bioucas-Dias, and A. Plaza, "Sparse unmixing of hyperspectral data," IEEE Trans. Geosci. Remote Sens., vol. 49, no. 6, pp.2014–2039, Jun. 2011.
[7] Z. Shi, W. Tang, Z. Duren, and Z. Jiang. "Subspace matching pursuit for sparse unmixing of hyperspectral data," IEEE Trans. Geosci. Remote Sens., vol.52, no.6, pp.3256-3274, Jun. 2013.
[8] J. M. Bioucas-Dias and M. A. T. Figueiredo, "Alternating direction algorithms for constrained sparse regression: Application to hyperspectral unmixing," in Proc. 2nd WHISPERS, Jun. 2010, pp. 1–4.
[9] M. D. Iordache, J. Bioucas-Dias, and A. Plaza, "Total variation spatial regularization for sparse hyperspectral unmixing", IEEE Trans. Geosci. Remote Sens., vol.50, no.11, pp. 4484-4502, Nov. 2012.
[10] M. D. Iordache, J. Bioucas-Dias and A. Plaza, "Collaborative sparse regression for hyperspectral unmixing", IEEE Trans. Geosci. Remote Sens., vol. 52, no. 1, pp.341-354, Jan. 2014.
[11] S. Cotter, B. Rao, K. Engan, K. Kreutz-Delgado, "Sparse solutions to linear inverse problems with multiple measurement vectors", IEEE Transactions on Signal Processing, vol.53, no.7, pp. 2477-2488, 2005.
[12] F. Kong, W. Guo, Y. Li, et al. "Backtracking-Based Simultaneous Orthogonal Matching Pursuit for Sparse Unmixing of Hyperspectral Data". Mathematical Problems in Engineering, 2015, 2015:1-17.